INTERNATIONAL JOURNAL OF AGRICULTURE & BIOLOGY
ISSN Print: 1560–8530; ISSN Online: 1814–9596
19F–059/2019/22–5–913–920
DOI: 10.17957/IJAB/15.1148
http://www.fspublishers.org

Full Length Article

Exploring the Mechanisms of Biosorption of Cr(VI) by Marine-Derived *Penicillium janthinellum* P1

Hui-Ying Chen[1*], Ya-Nan Lu[1], Ping-Chuan Yin[1], Xia Li[1*] and Yang Shan[2]
[1]*Guangxi Key Laboratory of Electrochemical and Magneto-chemical Functional Materials, College of Chemistry and Bioengineering, Guilin University of Technology, Guilin, 541004, China*
[2]*Hunan Agricultural Product Processing Institute, Hunan Academy of Agricultural Sciences, Changsha 410125, China*
[*]For correspondence: hychen@glut.edu.cn; biology754@163.com

Abstract

In this study, sorption of Cr(VI) by marine-derived fungus *Penicillium janthinellum* P1, well known for its multi-heavy-metal tolerance, was examined. First, Haplo-factor method was adopted to optimize key variables, such as temperature, incubation time, initial concentration, bio-sorbent dose and pH. The results showed that maximum Cr(VI) biosorption capacity for living fungus P1 pellets was about 87% at the optimum condition of beginning Cr(VI) concentration 250 mg/L, beginning pH 1, temperature of 30°C, biosorbent dosage of 30 g/L and contact time of 8 h, and that maximum Cr(VI) biosorption capacity for non-living fungus P1 pellets was about 58.6% at the optimum condition of beginning Cr(VI) concentration 100 mg/L, initial pH 1, temperature of 30°C, biosorbent dose of 3 g/L and contact time of 12 h. Then studies of kinetic, isotherm and thermodynamics were conducted to acquire an understanding of mechanisms of biosorption processes. The results demonstrated that the biosorption process of Cr(VI) ions followed pseudo-second order kinetic model, and that the biosorption process was fitted well to Freundlich, Dubinin-Radushkevich (D-R) isotherms. In addition, the calculation of thermodynamic parameters indicated that the biosorption of Cr(VI) on P1 pellets was feasible, spontaneous and endothermic. To decipher mechanisms of biosorption, Fourier Translation Infrared spectroscopy (FTIR), scanning electron microscope (SEM), X-ray photoelectron spectroscopy (XPS) and X-ray diffraction (XRD) analysis were further performed to investigate surface functional groups, cellular morphology and intracellular trace elements *etc*.

Keywords: Biosorption; Cr(VI); *Penicillium janthinellum*; XPS; XRD

Introduction

With the development of industry such as metallurgy, refractory materials, and chemicals, a large amount of chromium compounds have been exhausted into the environment, causing significant adverse biological and ecological impacts (Stasicka, 2000). It had been considered as a serious environmental pollutant. There are two stable oxidation situation of Cr(III) and Cr(VI) in the environment. Cr(III) is very different from Cr(VI) in terms of charge, chemical properties, biological activity and environmental impact. Cr(III) is considered to be essential for living organisms (Béni *et al.,* 2007), whereas Cr(VI) has more toxic effects than Cr(III) on biological systems (Gómez and Callao, 2006; Saleem *et al.*, 2018). Cr(VI) pollution has become a major concern worldwide. The general methods used for chromium-contaminated wastewater treatment include electro chemical method, chemical precipitation, evaporation and adsorption on activated carbon, *etc*. (Samuel and Chidambaram, 2015), which has its own limitation. Therefore, there is just an increasing and urgent demand to exploit more prompt removal steps for heavy metal mitigation.

Bioremediation is a non-destructive, economical and favorable clean-up technique that attempts to accelerate the naturally occurring biodegradation of pollution by optimizing constraints (Margesin and Schinner, 2001). Moreover, studies on biosorbents have indicated that both alive and dead microbial cells were able to adsorb metal ions and could be an alternative for common sorbents (Ting, 2001; Bano *et al.*, 2018). The adsorption characteristics of living cells are slow, irreversible and toxic by heavy metal, while those of non-living cells are fast, reversible and not affected by toxic ions. Owing to these differences, there is a different amount of adsorption of heavy metal ions between active and inactive cells, and this phenomenon needs further study.

Marine environments with extreme temperatures, low pH, high salinity, sea surface temperature, water flow, precipitation patterns and wind regimes are thought to be one of the most unfavorable environments. Due to the diversity of ecological conditions, marine microorganisms are more prone to adaptation to adverse conditions than those of terrestrial peers and had complex adaptive characteristics (Dash *et al.*, 2013). It had been reported that

To cite this paper: Chen, H.Y., Y.N. Lu, P.C. Yin, X. Li and Y. Shan, 2019. Exploring the mechanisms of biosorption of Cr(VI) by marine-derived *Penicillium janthinellum* P1. *Intl. J. Agric. Biol*., 22: 913–920

several marine microorganisms including bacteria, fungi, algae could be efficiently used as biosorbents (Dash *et al.*, 2013; Jayakumar *et al.*, 2014; Lu *et al.*, 2017). Not only had the fungi strong proliferative ability, but many fungi like *Penicillium* spp. and *Aspergillus sp.* also could form stable mycelia pellet for self-immobilization. This characteristic trait will facilitate subsequent removing procedure after adsorption. Hence, marine fungi with bioremediation potential can be an ideal candidate for biological treatment of contaminated extreme habitats.

According to our previous work (Chen *et al.*, 2014), marine-derived *Penicillium janthinellum* P1 had several excellent advantages, as follows i) strong multiple heavy metal and acid resistance; ii) strong adsorption capacity; iii) formation of mycelial pellets; iiii) rapid propagation. Allowing for these, in present study live and dead P1 both used as adsorbents, were used to remove Cr(VI) from solution. The influences of diverse operating variables on the sorption of Cr(VI) were investigated. Microorganisms have developed a variety of adsorption mechanisms, which may be one or a combination of transport across the cell membrane, physical adsorption, ion exchange, complexation, and precipitation (Beolchini, 1997; Ramirez-Diaz *et al.*, 2008). The analyses of the biosorption mechanisms of P1 pellets used thermodynamics, dynamics and equilibrium isotherms. Also, Fourier transform infrared (FT-IR), scanning electron microscope (SEM), X-ray diffraction (XRD) and X-ray photoelectron spectroscopy (XPS) were utilized to dissect the detoxifying mechanisms of cells in the response of heavy metal stress.

Materials and Methods

Biomass and Reagent Preparation

A 1 g/L concentration of Cr(VI) was equipped using double distilled water. A 0.2% diphenylcarbazide developer was prepared making use of double distilled water and acetone. The pre-activated P1 pellets was incubated into the PDA liquid medium at 30°C under shaking 120 $r \bullet min^{-1}$ for 7 days to obtain living cells. The cells were evenly divided into two portions, one of which was being inactivated at high temperature and pressure. All cells were freeze-dried at 4°C and then stored for later use.

Chromium Standard Curve

The chromium solution was formulated at concentrations ranging from 0–10 mg/L. In this experiment, hexavalent chromium was directly measured by diphenylcarbazide spectrophotometry. A blank spectrum was taken to ensure the distilled water and subtracted from all sample spectra.

General Experimental Procedures

A 50 mL working solution was used in all biosorption researches. The best biosorption for optimal removal of Cr(VI) in constantly stirred (120 rpm) flasks with contact time varying from 2–12 h, different initial pH (1–5), biomass dose (1–6 g/L) and beginning Cr(VI) concentration (25–125 mg/L) were verified. Independent experiments were conducted thrice, each in triplicates.

Removal Kinetics

So as to verify the mechanisms of sorption and dynamic interaction of Cr(VI) with P1 pellets, biosorptions of hexavalent chromium by P1 pellets biosorbent were tested using these kinetic models: pseudo-first-order, pseudo-second-order, Morris-Weber (Ho, 2004, 2006; Dissanayake *et al.*, 2016).

Pseudo-first order: $\log(q_e - q_t) = \log q_{eq} - \frac{K_1 t}{2.303}$ (1)

Pseudo-second order: $\frac{t}{q_t} = \frac{1}{K_2 q_e^2} + \frac{1}{q_e} t$ (2)

Intraparticle diffusion: $q_t = K_{id} t^{\frac{1}{2}}$ (3)

Equilibrium Sorption Isotherms

Generally, an sorption isotherm is an inestimable curve which depicts the reservation or fluidity of a nature from the aqueous perforated medium or aquatic circumstances to a solid-phase at a unchanging temperature and pH (Foo and Hameed, 2010). So far, many equilibrium isotherms have been established. The sorption mechanism of Cr(VI) on P1 pellets was researched by fitting the data from batch experiments with the Langmuir, Freundlich and Dubinin-Radushkevich isotherms. The equilibrium sorption isotherm models used to analyze these experimental data are listed in by the following equations (Langmuir I. The adsorption of gases on plane surfaces of glass, mica and platinum (Mittal *et al.*, 2010; Vieira *et al.*, 2018):

Langmuir isotherm: $\frac{1}{q_e} = \frac{1}{q_{max}} + \frac{1}{q_{max} b} \frac{1}{C_{eq}}$ (1)

Freundlich isotherm: $\log q_e = \log K_f + \frac{1}{n} \log C_{eq}$ (2)

D–R isotherm: $\ln q_e = \ln q_{max} - \beta \varepsilon^2$ (3)

Adsorption Thermodynamics

Further information on the natural energy and structural variation after sorption can be provided by a suitable assessment of thermodynamic parameters. Estimating change in Gibbs free energy (ΔG) could verify the feasibility and spontaneous essence of the process (Srivastava *et al.*, 2015). Calculation of thermodynamic parameters of sorption of Cr(VI) by fungal cells by the following equation

$$K_D = \frac{q_e}{C_e} \quad (1)$$

$$\triangle G = -RT \ln K_D \quad (2)$$

$$\triangle G=\triangle H-T\triangle S \quad (3).$$

Scanning Electron Microscope (SEM) Studies

The living cells and dead cells were respectively cultured at 150 rpm for 24 h in Cr(VI) concentrations of 0 mg/L, 100 mg/L. The cells were fixed overnight in a 2.5% glutaraldehyde solution at 4℃ and rinsed with phosphate buffer several times and fixed in 1% osmium tetroxide for 4 hours. It was subsequently dehydrated with ethanol and replaced with pure isocyanate for twice. The sample was then supercritically dried and coated with gold before it was examined by SEM (Hitachi S-520 scanning electron microscope, Japan).

Fourier Translation Infrared Spectroscopy (FTIR) Studies

So as to indicate the functional groups on the surface responsible for chromium biosorption, the resolution is 4 cm^{-1} in the spectral range of 500–4000 cm^{-1}, and the Cr(VI) concentrations is 0 mg/L, 100 mg/L, 150 mg/L, and 200 mg/L, respectively, FT-IR studies were implemented. The fungal cells were incubated with Cr(VI) synthetic solution at the above four concentration, and shaken at 150 rpm for 24 h. After vacuum freeze-drying, the samples were thoroughly ground and measured using a Nicolet 6700 Fourier Transform Infrared Spectrometer (FT-IR) with a resolution of 4 cm^{-1} and a scan extent of 4000–500 cm^{-1}.

X-ray Diffraction (XRD) Analysis

Live and dead cells cultured in the chromium-free and chromium-containing culture were vacuum dried and ground into a powder. The above sample powder was measured on a D8 Advance X-ray diffractometer and injected in a continuous scanning manner with a step width of 0.01° and 2 θ of 3°–70°.

X-Ray Photoelectron Spectroscopy (XPS)

The X-ray energy spectrum (XPS) can analyze the morphology and elementary changes of the cells before and after adsorption to determine the mechanism of chromium biosorption. The above sample powder was measured on an ESCALAB 250 spectrometer, and a monochromatic source of radiation (1486.6 eV) of A1 Kα was focused and scanned on a S-4800 ultra-high-resolution scanning electron microscope.

Results

Bisorption Experiments

Influence of pH: The influence of pH on the removal of Cr(VI) by the sorbents was inspected at initial pH levels of 1.00, 2.00, 3.00, 4.00 and 5.00, with other parameters constant. The experimental consequences were shown in Fig. 1a. The pH was in the range of 1 to 5, and the chromium removal rate decreased as the pH increased. The amount of Cr(VI) ions adsorbed by living cells was greater than that of dead cells.

Influence of contact time: Contact time was considered to be one of the most important factors affecting biosorption efficiency. Results on influence of contact time of Cr(VI) biosorption by living and dead cells of P1 pellets were shown in Fig. 1b. As shown in the Fig., the adsorption rate of living cells of P1 particles was rapid in the first 8 h, and then slowed down. The optimal adsorption time was 8 h. For dead cells, the optimal adsorption time was 12 hrs. And it was found that at these optimal time 66.4 and 42.3% of Cr(VI) were biosorbed by dead cells and live cells, respectively, after that the biosorption rate was decelerated. Dead cells were found to be more effective for hexavalent chromium adsorption compared to living cells.

Influence of biosorption dose: The influence of biosorption dose on the biosorption process was also considered as one of the most crucial elements that need to be solved and improved. With increase of biosorbent dosage, the biosorption capacity reduced from 22.1 mg/g to 9.27 mg/g for non-living cells, while for living cells, it shrank from 30.5 mg/g to 14.5 mg/g as biosorbent dose increased.

Influence of initial Cr(VI) ion concentration: The removal of chromium ions was investigated *via* the method of changing the initial Cr(VI) ion concentration. The experimental results are shown in Fig. 1d. For non-living P1 pellets, the biosorption of metal ions decreased with the enhancement of the initial concentration of Cr(VI) at the range of 50–150 mg/L. However, for living cells, during the initial concentration of 50–150 mg/L, metal ion uptake capacity gradually ascended at initial concentration up to 100 mg/L and when the initial concentration exceeded 100 mg/L, the adsorption of metal ions plummeted with the increase of the concentration of Cr(VI).

Influence of temperature: Fig. 1e showed the sorption and removal efficiency of Cr(VI) ions by P1 pellets under different temperature. removal rate of hexavalent chromium peaked at 30ºC. Overall, as the temperature rose to 40ºC, the removal rate of hexavalent chromium descended.

Kinetic Modeling

The results of three kinetic models used in this study were shown in Table 1. The adsorptions of Cr(VI) by both live and dead cells were in line with the pseudo-second-order kinetic model.

Equilibrium Isotherm Model

The correlation coefficients and parameters calculated by the isotherm model used in this study were listed in Table 2. As shown in Table 2, for both types of cells, the

Table 1: Biosorption kinetics parameters for the biosorption of Cr(VI) by P1 pellets

Cell type	Kinetic model	Pseudo-first order	Pseudo-second order	Intraparticle diffusion
Dead cells	Slope	-0.0010	0.0283	0.4262
	Intercept	1.2048	3.6632	17.3525
	k	2.303×10^{-3} L/mg	2.1863×10^{-4} g/mg/min	4.262×10^{-1} mg/g/min 0.5
	q_e	16.0225	35.3357	NA
	R^2	0.9782	0.9991	0.9063
Live cells	Slope	-0.0002	0.3041	0.0374
	Intercept	0.3154	97.803	0.9357
	k	2×10^{-4} L/mg	9.4554×10^{-4} g/mg/min	3.74×10^{-2} mg/g/min 0.5
	q_e	2.0673	3.2883	NA
	R^2	0.9761	0.9804	0.9834

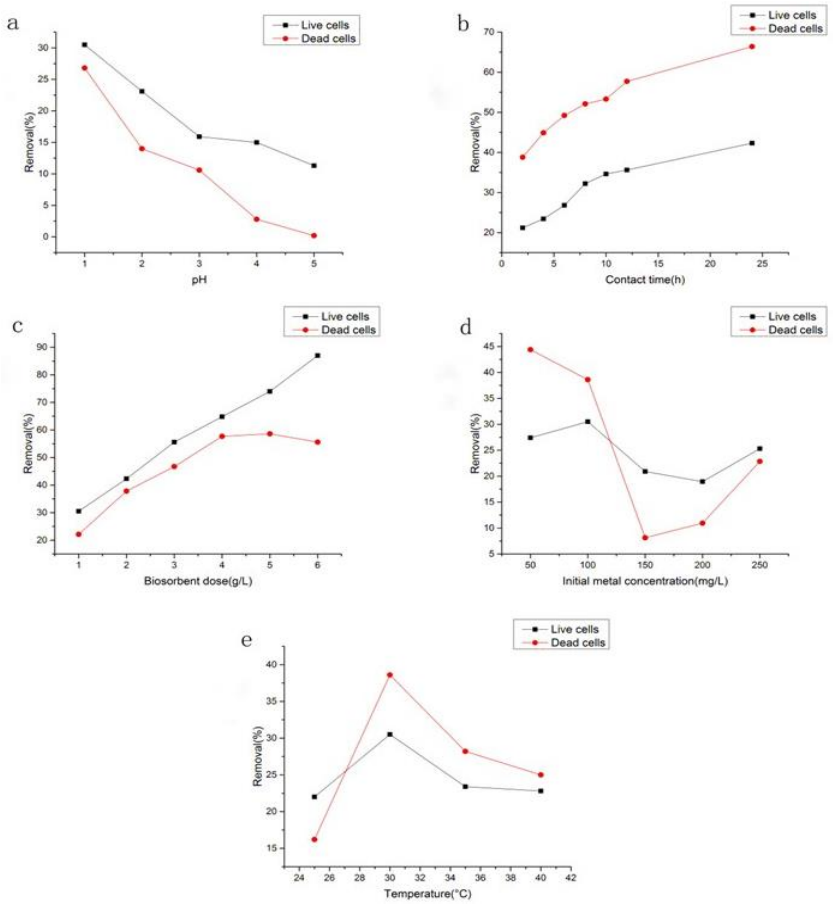

Fig. 1: Effect of various parameters initial pH (**a**), contact time (**b**), biosorbent dose (**c**), initial metal concentration (**d**) and temperature (**e**) on percentage removal of Cr(VI) onto P1 pellets

Langmuir isotherms didn't fit the experimental data because of low R^2 value, it was found by the isotherm fitting that the Langmuir isotherm model was not as apposite for the biosorption process as the Freundlich isotherm model (R^2=0.96 for live cells, R^2=0.98 for dead cells). The energy value obtained from viable cell (Table 2) was less than 8 kJ/mol, revealing that the sorption of Cr(VI) by living cell was a physical process, whereas the biosorption of Cr(VI) by dead cell whose energy value was more than 8 kJ/mol was a chemical process.

Thermodynamic Studies

The positive values of ΔS (244.77 kJ/mol) suggested that the large degree of chaos in the solid/dissolved interface occurred during the sorption process. Positive values of ΔH (75335.80 kJ/mol) indicated the endothermic property of the sorption. The negative value of ΔG decreased with increase of temperature, and its value changed from negative to positive, showing that the spontaneous essence of sorption was inversely proportional to temperature.

Table 2: Equilibrium isotherm parameters for the biosorption of Cr(VI) onto P1 pellets

Isotherms	Live cells	Dead cells
Langmuir		
q_{max}	-4.7449	2.3397
R_L	<1	<1
R^2	0.3759	0.8384
Freundlich constant		
K_f	2.60×10^{-6}	0.9708
n	8.76×10^{-2}	5.7339
R^2	0.9683	0.9819
D–R isotherms		
E	0.158	438.8
q_{max}	2.15×10^{3}	1.1153×10^{3}
R^2	0.9852	0.9960

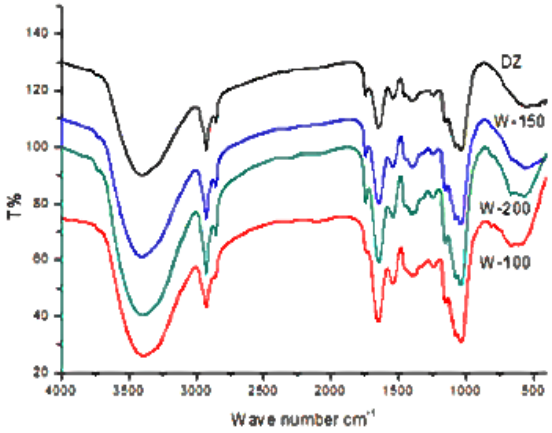

Fig. 2: FTIR spectra of native P1 pellets (DZ), 100 mg/L Cr(VI) loaded P1 pellets (W-100), 150 mg/L Cr(VI) loaded P1 pellets (W-150), and 150 mg/L Cr(VI) loaded P1 pellets (W-200)

Characterization of Biosorbents

FTIR analysis: The FT-IR spectra were shown in Fig. 2. The spectra of the biosorbents had a wide range of sorption peaks spanned from 3500–3300 cm^{-1}. There was a stretching vibration of O-H and N-H of polysaccharides, indicating hydroxyl groups or amino groups interacted with Cr(VI). There was a stretching vibration absorption of SP_3 hybridized C-H at 2950 to 2850 cm^{-1}. Both peaks were formed by a slight red shift of the spectrum of the biosorbent without adsorbed Cr(VI). There were a C-O stretching vibration absorption peak at 1800–1600 cm^{-1}, and a SP_3 hybrid C-O stretching vibration characteristic absorption peak at 1100–1000 cm^{-1}.

SEM analysis: The surface structure and particle size distribution of P1 pellets before and later adsorption of Cr(VI) were presented in the SEM photographs. By observing an enlarged view of the SEM micrograph shown in Fig. 3, it was found that the surfaces of P1 pellets before biosorption of chromium were fuller and shinier than those of after adsorption. After the adsorption of chromium ions, there were bright spots scattered on the surface of the hyphae, indicating that a large amount of chromium ions were adsorbed on the cell surface.

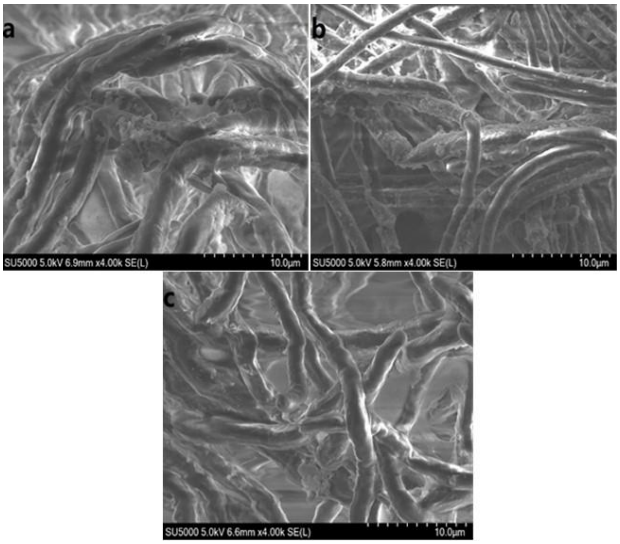

Fig. 3: SEM images of 100 mg/L Cr(VI) loaded dead P1 pellets (**a**), 100 mg/L Cr(VI) loaded living P1 pellets (**b**), native P1 pellets (**c**)

XRD analysis: Compared with the spectrum before adsorption, the spectrogram after adsorption of chromium ions had no obvious peak diffraction line, and the diffraction peaks overlapped, indicating that there might be no crystal structure on the surface of the cells. XRD patterns showed that no crystal forms of Cr existed on the surface of the biomaterial after the treatment.

XPS analysis: XPS spectrum was picked from the Cr 2p main areas of the cells after adsorption of chromium ions and the cells of the blank control (Fig. 4). As shown in Fig. 4, the peaks with binding energy of 576.98 eV and 586.48 eV represented the ribbons of standard Cr(III) compounds. As shown in Fig. 5, in the spectrum of C_{1s}, the peak with a binding energy of 284.38 eV represented the C-C or C-H bond; the peak with a binding energy of 285.88 eV was the C-O bond in alcohol, ether or phenol; the peak with a binding energy of 288.38 eV represented the C=O or O-C=O bonds in the ketone, ester or carboxyl group. The spectra of the C element on the surface of cells after adsorption of Cr were shown in Fig. 5c and d.

Discussion

The pH and chromium ion concentration in the solution determined the relative abundance of Cr(VI) (Sari and Tuzen, 2008). It was deduced that $HCrO4^-$ was the predominant form of Cr(VI) at pH 1–2. For living cells, as the pH of the solution increased, the number of negatively charged sites increased and the sites of positive charge on the biosorbent surface decreased. Studies had shown that the pH can influence the biosorption process by affecting the growth of the strain,

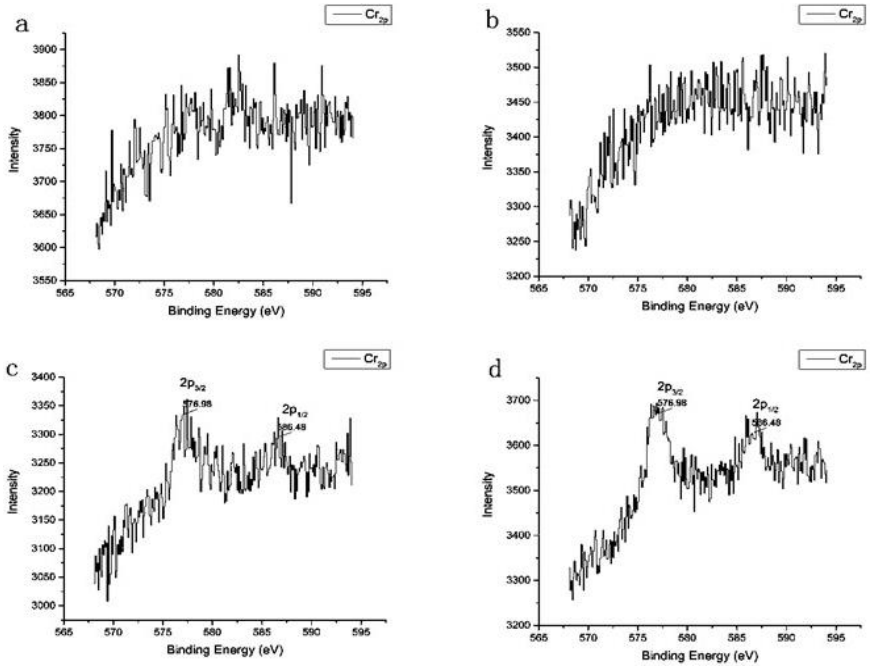

Fig. 4: XPS spectra of Cr2p of living P1 pellets (**a**), dead P1 pellets (**b**), Cr(VI) loaded living P1 pellets (**c**) and dead P1 pellets (**d**)

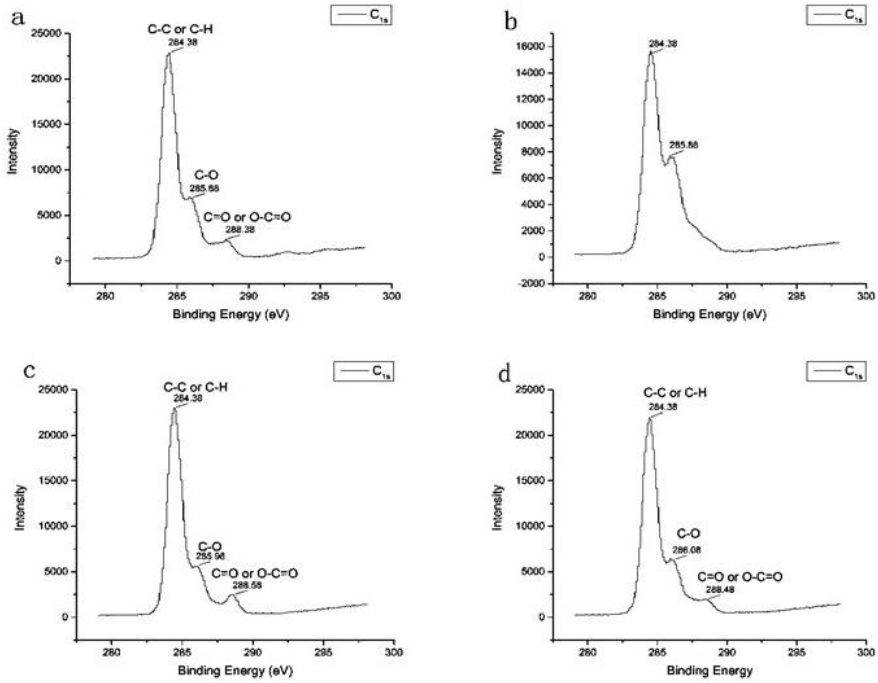

Fig. 5: XPS spectra of C1s of living P1 pellets (**a**), dead P1 pellets (**b**), Cr(VI) loaded living P1 pellets (**c**) and dead P1 pellets (**d**)

the property of the adsorption site, and the state of heavy metal ions in the solution (Kiran *et al.*, 2006). Because the cell surface had numerous negatively charged functional groups, the amount of Cr(VI) ion which viable cells adsorbed was greater than that of dead cells.

The results clearly demonstrated that P1 had two steps in the sorption of Cr(VI) ions. The first step was a rapid apparent adsorption, and another one was a slow intercellular diffusion until equilibrium was established (Bhatti *et al.*, 2010). Bioaccumulation was that metal ions were first bound to the cell surface, and then accumulated in the cells, whereas physicochemical process or ion exchange

may occur in bioaccumulation. Therefore, biosorption was faster than bioaccumulation (Chojnacka, 2010). Owing to absence of active metabolisms in dead cells, the large increase of surface area of non-living cells led to a great number of adsorption sites associated with bioaccumulation.

With increase of biosorbent dosage, removal of Cr(VI) was escalated. This may be due to enhancement of surface area of the adsorbent, resulting in increase of binding site at the sorbent surface for the metal ion (Rocha *et al.*, 2013). With continuous increase of biosorbent dose, the partial aggregation of adsorbent would occur, which caused the effective surface area of biosorption to shrink, eventually leading to a reducing at the removal rate of Cr(VI) (Karthikeyan *et al.*, 2007).

Fig. 1d indicated that the amount of biosorption and Cr(VI) ion removal rate also varied with solution concentration. It was obvious that a gradual decrease in balance sorption containment was accompanied by an enhancement of initial Cr(VI) ion concentration. After reaching a certain concentration, the amount of adsorption maintained a certain equilibrium state. The active sites of the adsorbent became saturated at a certain Cr(VI) ion concentration because of its limited amount. The decrease in the rate of initiation of external diffusion and the increase in the rate of diffusion within the particle are due to an increase in the concentration of the beginning metal ion (Nemr *et al.*, 2008).

Within a certain temperature range, as the culture temperature increased, the growth and reproduction of microorganisms and metabolic activities were strengthened, and the rate of reduction of Cr(VI) was also accelerated. When the ambient temperature exceeded 30°C, it would be detrimental to the cells. The removal of Cr(VI) reduced as the temperature raised to 40°C, which indicated that a low temperature favored Cr(VI) biosorption. Temperature had two main influences on the biosorption process. The first effect was that the increase in temperature caused the viscosity of the solution to decrease, increasing the rate into which biosorbed molecules diffused the outer boundary layer and the internal pores of the biosorbent particles. The second was possible that the balance containment of the sorbent for a particular sorbate changed with temperature (Barka *et al.*, 2013).

Sorption kinetics was decided by the following four steps: (1) external diffusion; (2) internal diffusion; (3) surface diffusion; and (4) surface reaction (Dąbrowski, 2001). The adsorptions of Cr(VI) by both live and dead cells were in adaptation with the pseudo-second-order kinetic model. The rates of chemical reaction between the functional groups on the cell surface and Cr(VI) determined the rate of adsorption of Cr(VI) by living cells and dead cells. The kinetic results showed that the rate of chemical reaction between the functional groups on the cell surface and Cr(VI) determined the rate of adsorption of Cr(VI) by living cells and dead cells. Further analysis showed that q_t and $t_{1/2}$ were linearly fitted. The absence of a straight line through the origin indicated that intraparticle diffusion was not the sole rate limiting step in the sorption process.

Adsorption isotherms, which elucidated the relationship between the adsorbate and the adsorbent, were crucial for the optimization of the adsorption pathway, indication of the surface properties and capacity of the adsorbent (Kyzas and Matis, 2015). The nonideality sorption and multi-layer adsorption mode of Cr(VI) mainly adsorbed on heterogeneous surfaces were found by isotherm fitting. The energy value revealed that the sorption of Cr(VI) by living cells was a physical process, whereas the biosorption of Cr(VI) by dead cells was a chemical process. In summary, the adsorption mechanism of living cells was more complicated than that of dead cells. The surface active site on the biosorbent may result in increase of adsorption with temperature (Jayakumar *et al.*, 2014).

The FTIR spectrum of the sorbent and sorbent adsorbing metal ions were contrasted to decide which functional groups on the surface of the adsorbent were involved in the adsorption of Cr(VI). By analyzing the characteristic peaks on the infrared spectrum, the presence of amino, carboxyl, carbonyl, and hydroxyl groups on the surface of P1 was found. The interaction of these four functional groups on the surface of P1 with the above ions was verified by changes in the position of the band before and after biosorption.

The morphology of the cells after the chromium ion treatment was not destroyed. The cells were filamentous which intertwined to form a network. Due to this characteristic structure, P1 pellets had an outstanding ability to sorb and remove chromium.

In Fig. 4 first peak corresponded to Cr $2p_{3/2}$ orbital, and the second one corresponded to Cr $2p_{1/2}$ orbital (Park *et al.*, 2008). Thence, it can be possibly determined that P1 pellets achieved the purpose of removing Cr(VI) by reducing Cr(VI) in the aqueous solution to Cr(III). After the interaction of P1 pellets with Cr(VI), the relative area of C-O bond decreased slightly, and the binding energy increased slightly, which indicated that the Cr(III) reduced by Cr(VI) reacted with the functional groups on the surface to form ether-Cr(III) or R-O-Cr(III) complex species. The relative area of C=O or O-C=O bond enhanced, and the binding energy also increased, indicating that C=O or O-C=O bond participated in the adsorption of Cr(III) and formed carboxyl-Cr(III) complex species (Liu *et al.*, 2013). The relative area and high binding energy of the C-C or C-H bond indicated that much more hydrogen-containing functional groups were produced on the surface during the reduction and adsorption of the cells (Liu *et al.*, 2012).

Conclusion

The above experiments demonstrated that the sorption of chromium ions by living cells was more complicated than that of dead cells. FT-IR and XPS spectroscopy analysis showed that amino groups, carboxyl groups, hydroxyl

groups and C-H bond on the surface of the cells played critical roles for P1 pellets in adsorbing Cr(VI) ions to the surfaces to form organic chromium. Additionally, oxidation-reduction mechanism, in which Cr(III) was reduced by Cr(VI) and then formed a series of Cr(III)-related complex substances, was involved in biosorption and detoxifying processes. In conclusion, *P. janthinillum* P1 biosorbent had a great potential for the treatment of Cr(VI) in wastewater.

Acknowledgement

This research was financially supported by the National Natural Science Foundation of China (Nos. 21762015, Nos. 31860251), the Guangxi Education Department Project (2017KY0251), the Guangxi Key Laboratory of Electrochemical and Magneto-chemical Functional Materials (EMFM20162203). Research Program of Guangxi Specially-invited Experts (Key technologies for intensive processing and quality safety of agricultural products, TingFa[2018]39).

References

Bano, A., J. Hussain, A. Akbar, K. Mehmood, M. Anwar, M.S. Hasni, S. Ullah, S. Sajid and I. Ali, 2018. Biosorption of heavy metals by obligate halophilic fungi. *Chemosphere*, 199: 218–222

Barka, N., M. Abdennouri, M.E. Makhfouk and S. Qourzal, 2013. Biosorption characteristics of cadmium and lead onto eco-friendly dried cactus (*Opuntia ficus* indica) cladodes. *J. Environ. Chem. Eng.*, 1: 144–149

Béni, Á., R. Karosi and J. Posta, 2007. Speciation of hexavalent chromium in waters by liquid–liquid extraction and GFAAS determination. *Microchem. J.*, 85: 103–108

Beolchini; F.V.F., 1997. Removal of metals by biosorption: a review. *Hydrometallurgy*, 44: 301–316

Bhatti, H.N., A.W. Nasir and M.A. Hanif, 2010. Efficacy of *Daucus carota* L. waste biomass for the removal of chromium from aqueous solutions. *Desalination*, 253: 78–87

Chen, H.Y., Y.X. Guan and S.J. Yao, 2014. A novel two-species whole-cell immobilization system composed of marine-derived fungi and its application in wastewater treatment. *J. Chem. Technol. Biotechnol.*, 89: 1733–1740

Chojnacka, K., 2010. Biosorption and bioaccumulation-the prospects for practical applications. *Environ. Intl.*, 36: 299–307

Dąbrowski, A., 2001. Adsorption from theory to practice. *Adv. Colloid Interface Sci.*, 93: 135–224

Dash, H.R., N. Mangwani, J. Chakraborty, S. Kumari and S. Das, 2013. Marine bacteria: potential candidates for enhanced bioremediation. *Appl. Microbiol. Biotechnol.*, 97: 561–571

Dissanayake, D.M.R.E.A., W.M.K.E.H. Wijesinghe, S.S. Iqbal, N. Priyantha and M.C.M. Iqbal, 2016. Isotherm and kinetic study on Ni(II) and Pb(II) biosorption by the fern *Asplenium nidus* L. *Ecol. Eng.*, 88: 237–241

Foo, K.Y. and B.H. Hameed, 2010. Insights into the modeling of adsorption isotherm systems. *Chem. Eng. J.*, 156: 2–10

Gómez, V. and M.P. Callao, 2006. Chromium determination and speciation since 2000. *TrAC Trends Anal. Chem.*, 25: 1006–1015

Ho, Y.S., 2006. Second-order kinetic model for the sorption of cadmium onto tree fern: A comparison of linear and non-linear methods. *Water Res.*, 40: 119–125

Ho, Y.S., 2004. Citation review of Lagergren kinetic rate equation on adsorption reactions. *Scientometrics*, 59: 171–177

Jayakumar, R., M. Rajasimman and C. Karthikeyan, 2014. Sorption of hexavalent chromium from aqueous solution using marine green algae *Halimeda gracilis*: Optimization, equilibrium, kinetic, thermodynamic and desorption studies. *J. Environ. Chem. Eng.*, 2: 1261–1274

Karthikeyan, S., R. Balasubramanian and C.S. Iyer, 2007. Evaluation of the marine algae *Ulva fasciata* and *Sargassum* spp. for the biosorption of Cu(II) from aqueous solutions. *Bioresour. Technol*., 98: 452–455

Kiran, I., T. Akar, A.S. Ozcan, A. Ozcan and S. Tunali, 2006. Biosorption kinetics and isotherm studies of Acid Red 57 by dried *Cephalosporium aphidicola* cells from aqueous solutions. *Biochem. Eng. J.*, 31: 197–203

Kyzas, G.Z. and K.A. Matis, 2015. Nanoadsorbents for pollutants removal: A review. *J. Mol. Liquids*, 203: 159–168

Liu, H., Q. Gao, P. Dai, J. Zhang, C. Zhang and N. Bao, 2013. Preparation and characterization of activated carbon from lotus stalk with guanidine phosphate activation: Sorption of Cd(II). *J. Anal. Appl. Pyrol.*, 102: 7–15

Liu, H., X. Wang, G. Zhai, J. Zhang, C. Zhang, N. Bao and C. Cheng, 2012. Preparation of activated carbon from lotus stalks with the mixture of phosphoric acid and pentaerythritol impregnation and its application for Ni(II) sorption. *Chem. Eng. J.*, 209: 155–162

Lu, T., Q. Zhang and S. Yao, 2017. Efficient decolorization of dye-containing wastewater using mycelial pellets formed of marine-derived *Aspergillus niger*. *Chin. J. Chem. Eng.*, 25: 330–337

Margesin, R. and F. Schinner, 2001. Biodegradation and bioremediation of hydrocarbons in extreme environments. *Appl. Microbiol. Biotechnol.*, 56: 650–663

Mittal, A., J. Mittal, A. Malviya, D. Kaur and V.K. Gupta, 2010. Decoloration treatment of a hazardous triarylmethane dye, Light Green SF (Yellowish) by waste material adsorbents. *J. Colloid Interface Sci.*, 342: 518–527

Nemr, A.E., A. Khaled, O. Abdelwahab and A. El-Sikaily, 2008. Treatment of wastewater containing toxic chromium using new activated carbon developed from date palm seed. *J. Hazard. Mater.*, 152: 263–275

Park, D., Y.S. Yun, H.W. Lee and J.M. Park, 2008. Advanced kinetic model of the Cr(VI) removal by biomaterials at various pHs and temperatures. *Bioresour. Technol.*, 99: 1141–1147

Ramirez-Diaz, M.I., C. Diaz-Perez, E. Vargas, H. Riveros-Rosas, J. Campos-Garcia and C. Cervantes, 2008. Mechanisms of bacterial resistance to chromium compounds. *Biometals.*, 21: 321–32

Rocha, L.S., C.B. Lopes, J.A. Borges, A.C. Duarte and E. Pereira, 2013. Valuation of unmodified rice husk waste as an eco-friendly sorbent to remove mercury: A study using environmental realistic concentrations. *Water Air Soil Pollut.*, 224: 1599

Saleem, M.U., H.N. Asghar, Z.A. Zahir and M. Shahid, 2018. Integrated effect of compost and Cr^{6+} reducing bacteria on antioxidant system and plant physiology of alfalfa. *Intl. J. Agric. Biol*., 20: 2745–2752

Samuel, M.S. and R. Chidambaram, 2015. Hexavalent chromium biosorption studies using *Penicillium griseofulvum* MSR1 a novel isolate from tannery effluent site: Box–Behnken optimization, equilibrium, kinetics and thermodynamic studies. *J. Taiwan Inst. Chem. Eng.*, 49: 156–164

Sari, A. and M. Tuzen, 2008. Biosorption of total chromium from aqueous solution by red algae (*Ceramium virgatum*): equilibrium, kinetic and thermodynamic studies. *J. Hazard. Mater.*, 160: 349–355

Srivastava, S., S.B. Agrawal and M.K. Mondal, 2015. Biosorption isotherms and kinetics on removal of Cr(VI) using native and chemically modified *Lagerstroemia speciosa* bark. *Ecol. Eng.*, 85: 56–66

Stasicka, J.K.Z., 2000. Chromium occurrence in the environment and methods of its speciation. *Environ. Pollut.*, 107: 263–283

Ting, K.M.K.Y.P., 2001. Biosorption of gold by immobilized fungal biomass. *Biochem. Eng. J.*, 8: 51–59

Vieira, J.C., L.C. Soares and R.E.S. Froes-Silva, 2018. Comparing chemometric and Langmuir isotherm for determination of maximum capacity adsorption of arsenic by a biosorbent. *Microchem. J.*, 137: 324–328

[Received 18 Mar 2019; Accepted 08 May 2019; Published (online) 10 Nov 2019]